Use of Ground Penetrating Radar for Determination of Water Table Depth and Subsurface Soil Characteristics at Kennedy Space Center

Gideon M. Hengari[1,2], Carlton R. Hall[1], Tim J. Kozusko[1], Charles R. Bostater[2,*]

[1]InoMedic Health Application, Kennedy Space Center, FL 32899

[2] College of Engineering, Marine Environmental Optics Laboratory & Remote Sensing Center, Florida institute of Technology, 150 West University Blvd., Melbourne, Florida, USA

ABSTRACT

Sustainable use and management of natural resources require strategic responses using non-destructive tools to provide spatial and temporal data for decision making. Experiments conducted at John F. Kennedy Space Center (KSC) demonstrate ground penetrating radar (GPR) can provide high-resolution images showing depth to water tables. GPR data at KSC were acquired using a MALÅ Rough Terrain 100 MHz Antenna. Data indicate strong correlation (R^2=0.80) between measured water table depth (shallow monitoring wells and soil auger) and GPR estimated depth. The study demonstrated the use of GPR to detect Holocene and Pleistocene depositional environments such as Anastasia Formation that consists of admixtures of sand, shell and coquinoid limestone at a depth of 20-25 ft. This corresponds well with the relatively strong reflections from 7.5 to 13 m (125-215 ns) in GPR images. Interpretations derived from radar data coupled with other non-GPR data (wells data and soil auger data) will aid in the understanding of climate change impacts due to sea level rise on the scrub vegetation composition at KSC. Climate change is believed to have a potentially significant impact potential on near coastal ground water levels and associated water table depth. Understanding the impacts of ground water levels changes will, in turn, lead to improved conceptual conservation efforts and identifications of climate change adaptation concepts related to the recovery of the Florida scrub jay (*Aphelocoma coerulescens*) and other endangered or threatened species which are directly dependent on a healthy near coastal scrub habitat. Transfer of this inexpensive and non-destructive technology to other areas at KSC, Florida, and to other countries, may prove useful in the development of future conservation programs.

Keywords: Ground Penetrating Radar, Megahertz, Rough Terrain Antenna, dielectric constant, Anastasia Formation, Spodic Horizon, Holocene, Pleistocene

1. INTRODUCTION

Climate change coupled with several human induced factors, such as unsustainable utilization of the natural resources and habitat degradation, resulted in endangerment and extinction of numerous species of fauna and flora. One way to ensure sustainable restoration of degraded habitats is to consider several factors such as vegetation distribution and abundance, surface and subsurface soil characteristics, and subsurface water depth. Authors such as [2],[3],[4] emphasized the importance of water table dynamics on plant species composition and distribution in different temperate zones and wetlands. Efforts to restore habitat endangered flora and fauna utilize non-destructive tools to provide spatial and temporal data for decision making. Remote sensing has been the fundamental tool used in determining some of the biophysical and biochemical variables for monitoring and research [5]. Use of airborne and satellite remote sensing works well in detecting bio-chemical, bio-physical attributes at the leaf and canopy level. Assessment of subsurface attributes necessary for vegetation monitoring are limited using airborne and satellite remote sensing. Thus ground penetrating radar (GPR) is applied to characterize shallow subsurface features at scales from centimeters to kilometers [6]. The GPR technique is similar to seismic surveying. One antenna (the transmitter) radiates short pulses of high-frequency electromagnetic waves, while the other antenna (the receiver) measures the signal from the transmitter as a function of time [6]. GPR uses both active and passive remote sensing systems to transmit and record energy backscattered when the waves encounter an interface between materials with different dielectric permittivity.

[*]contact information Charles Bostater cbostate@fit.edu

Earth Resources and Environmental Remote Sensing/GIS Applications IV, edited by Ulrich Michel, Daniel L. Civco, Karsten Schulz, Manfred Ehlers, Konstantinos G. Nikolakopoulos, Proc. of SPIE Vol. 8893, 889318 · © 2013 SPIE · CCC code: 0277-786X/13/$18 · doi: 10.1117/12.2030023

The work presented here investigates the applicability of (GPR) in determination of water-table depth and associated subsurface soil characteristics at John F. Kennedy Space Center (KSC). GPR has been extensively used to map the shallow subsurface features due to its relatively high resolution [7]. The applicability of GPR is based on electromagnetic characteristics of materials, the dielectric constant of liquid water and that of other subsurface features under consideration [7].

2. AQUISITION OF GPR IMAGERY

Tel-4 area at (KSC) was chosen to be suitable for GPR imaging because of monitoring wells installed in the area, this allowed validation of GPR images. Topography of the area ranges between 1-3 m above sea level and scrub oak ridge on the highest elevation forms a continuous line in Tel-4 [8]. The topography is marked by a sequence of ridges and swales reflecting relict beach ridges. The ProEx (Professional Explorer Control Unit) GPR system (with MALÅ Rough Terrain 100 MHz Antenna (RTA) as shown in Figure 1 below was used to determine the spatial and temporal variability of water table depth at John F. Kennedy Space Center (KSC). The RTA can be maneuvered in any type of the environment including the densely vegetated was chosen to be an appropriate antenna.

Figure 1. GPR system (ProEx unit and the RTA antenna).

Defined by [9] as "a measure of the material (vegetation, soil, rock, water, ice) to conduct electrical energy" dielectric constant is fundamental parameter in the GPR system. Dielectric constant influences the propagation velocity of electromagnetic waves through a material, and it is known to affect horizontal imaging resolution [10]. Magnetic permeability also influences the velocity of the propagating waves in the soil, but most soils have negligible variation in magnetic permeability making dielectric constant the most significant impact on the recorded GPR response [11]. Water has a high dielectric constant of ≈81 as shown in table 1, therefore, radar waves travel more slowly in wet materials than dry ones [12]. On the other hand, dry materials have dielectric constants from 3 to 8 [9]; propagation can vary within a soil type depending on local conditions of moisture content and material structure [9]. From the Table 1 below it can be seen that the larger value given for velocity applies to unsaturated media. These values given, are only approximate, and can vary greatly with the water content in the medium.

Table 1. Dielectric constants and velocity of waves in different mediums adapted from [3].

Material	Dielectric constant	Velocity (m/ns)
Air	1	300
Fresh water	81	33
Limestone	7-16	75-113
Schist	5-15	77-134
Clay	4-16	74-150
Silt	9-23	63-100
Sand	4-30	55-150

3. FIELD METHODS

A selected portion of the area where there are monitoring shallow wells installed to monitor changes in depth to water table at Tel-4 was surveyed. We conducted soil excavations with soil a auger at selected points along each transect to validate observations on the GPR profile, and also to substantiate measured depth to water table. GPR was dragged along the identified transect, and also close to monitoring wells installed in the area in order to map the subsurface features. Depth to water-table from selected wells was also manually determined using a pressure sensitive data logger. This was further used for validation of the GPR estimated water table depth and water-table depth from the soil auger methodology. For the soil auger methodology, three random sampling points were identified within each of the GPR transects. Two of the points were on the ridge, and one was close to the swale as shown in Figure 2. At each sampling point, the auger was bored through the soil at each interface later identified (Soil auger points represented by solid blue dots on the image below). Eleven GPR surveys were completed at intervals of 4 to 6 weeks over a 6 month period. The Rough Terrain Antenna was dragged continuously along the selected three paths (indicated by solid blue lines in the figure below) to acquire the GPR data. The start to end positions of these profiles were recorded using a Trimble Navigation Pathfinder Professional XL GPS unit. This device allowed exact identification of the area surveyed on the GIS images of Tel-4 as shown in the figure below.

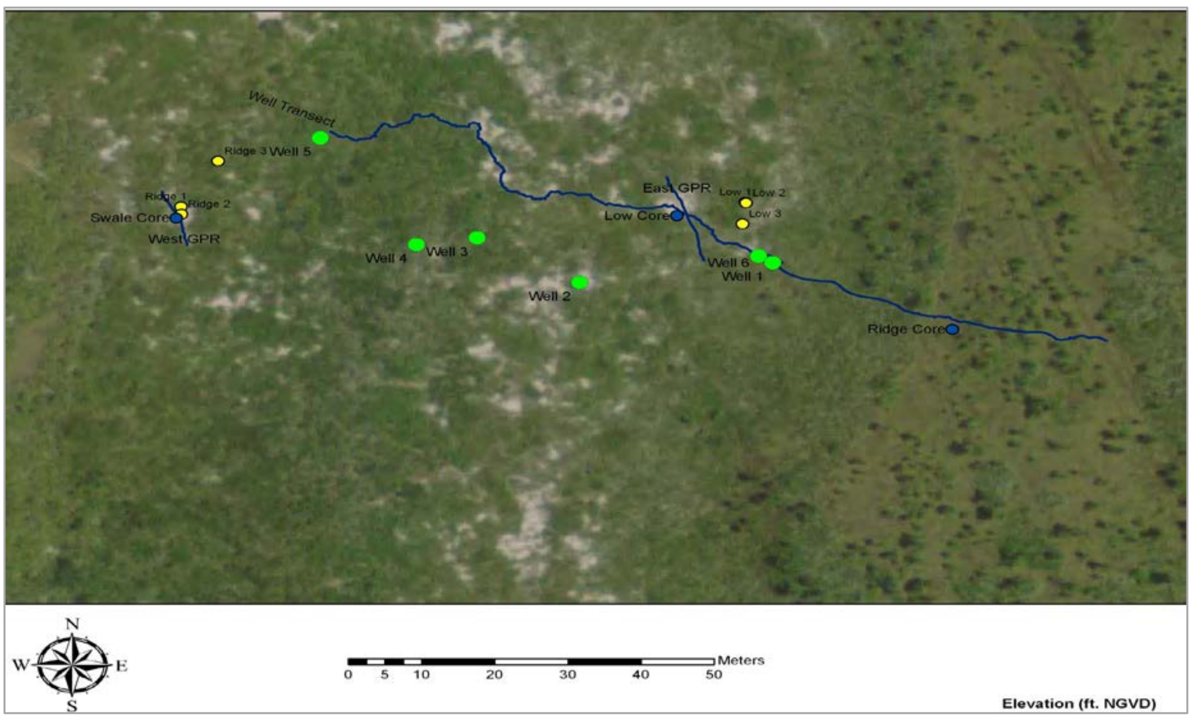

Figure 2. Location of monitoring shallow wells and GPR paths.

4. DATA ANALYSIS PROCEDURE

GPRSoft software from the GeoScanners AB was used for the GPR data processing. Like any remote sensing data, the GPR raw data contained interference from the external objects and subsurface discontinuities in the form of noise [14]. Some of the electromagnetic energy passes directly from a transmitting to receiving antenna through the air without being in conduct with medium, and can significantly affect GPR imaging [11]. Before any interpretation of the images, several processing techniques using the GPRSoft software were used and are summarized below (RadExplorer, and GPRSoft software manuals):

- A surface correction was the first step in the processing of the GPR images, because of the airwave and other external objects (e.g. plants branches) the GPR system on several occasions failed to detect the precise zero time of the profile.
- Background removal was the next in the processing of the GPR images. This was used to remove any instrument noise that blocked the desired signal [14]. These GPR signals were analyzed in the frequency spectrum and the band pass filters were used to remove the noise [15].
- The post-processing also included the application of automatic gain control (AGC) function to make low-amplitude signals more visible.
- The GPR was de-wowed to remove low frequency components from the data associated with electromagnetic induction or instruments range dynamic limitations [15].

The two-way travel time associated with an electromagnetic wave traveling between a radar transmitter and receiver through the medium was used to estimate the dielectric permittivity of the soil. This was used to verify the water table depth obtained from the shallow wells installed at Tel-4 and from the soil auger method. The following equation was used to determine the velocity of the wave propagating into the medium which later allowed for computation of dielectric permittivity or depth to the medium under consideration.

The wave velocity (V) propagating in any medium of known dielectric constant is given by [7]:

$$V = c/\sqrt{\varepsilon} \ , \quad (1)$$

Where, c is the speed of light in vacuum (0.3 m/ns) and Ɛ is the relative permittivity of the soil or the dielectric constant. The total or the two-way travel time (ns) was calculated from the following formula because the depth to the water table in the area was determined prior to the GPR measurements [7]:

$$\tau = \frac{2d}{v} \ , \ \frac{2d\sqrt{\varepsilon}}{c} \ , \quad (2)$$

If the velocity of the propagating waves through the medium is known, the two-way travel time usually measured in nanoseconds can be used to calculate the depth (d) of the medium.

5. RESULTS AND DISCUSSION

For all GPR profiles collected, the vertical scale is presented as a two-way travel time in nanoseconds (ns) and is on the left hand side of the profile; the horizontal scale is distance in meters (m). The depth scale is in meters (m) and is shown on the right hand side of the profile. Results indicate that GPR can provide good images that clearly indicate depth to water table and some geologic features associated with Pleistocene and Holocene formations. Figure 3 below shows radar responses that indicate the depth to the water table (indicated by solid blue line). From the Figure below, the water table doesn't provide strong and continuous amplitude or clear boundaries between the surface and the water table depth. The end of the strong reflection at 1.5-2 m was interpreted as the water table depth and it correlated well with the well data. Strength of the water-table radar reflector is largely influenced by the contrast between the electrical properties of the unsaturated and saturated zones [16]. In our study, water table depth calibrations were based on measured depths to the water table in shallow monitoring wells. The disparity had little effect and assisted in validating the accuracy of radar interpreted water-table depths.

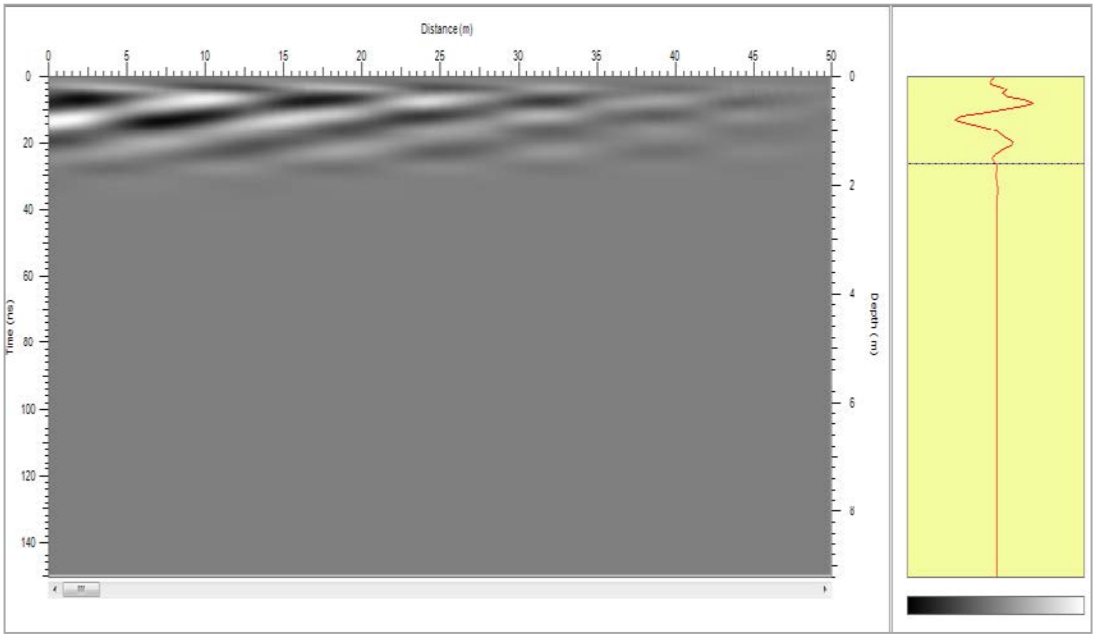

Figure 3. GPR profile from the top of the ridge (highest elevation), profile trimmed to 8 m.

Figure 4 shows the same radar response as in previous figure (not trimmed to 8 m) with two distinct layers. Another very prominent reflection in the radar response is at 7.5 to 13m (125-215 ns) as indicated by the black rectangle. The distinct reflection was interpreted as the Anastasia formation which can be predominantly found along the eastern coastline of Florida. Around the study area the surficial deposits from Merritt Island and Cape Canaveral are of Pleistocene and Recent ages and consist primarily of sand and sandy coquina [1]. Pleistocene deposits on Merritt Island are sometimes mapped as the Anastasia formation of high energy beach [1]. The Anastasia Formation consists of various admixtures of sand, shell, and coquinoid limestone. [1] conducted a study at Kennedy Space Center and found the Anastasia formation at the depth from 20-25 ft, which corresponds very well with the relatively strong reflections from 7.5 to 13m (125-215 ns).

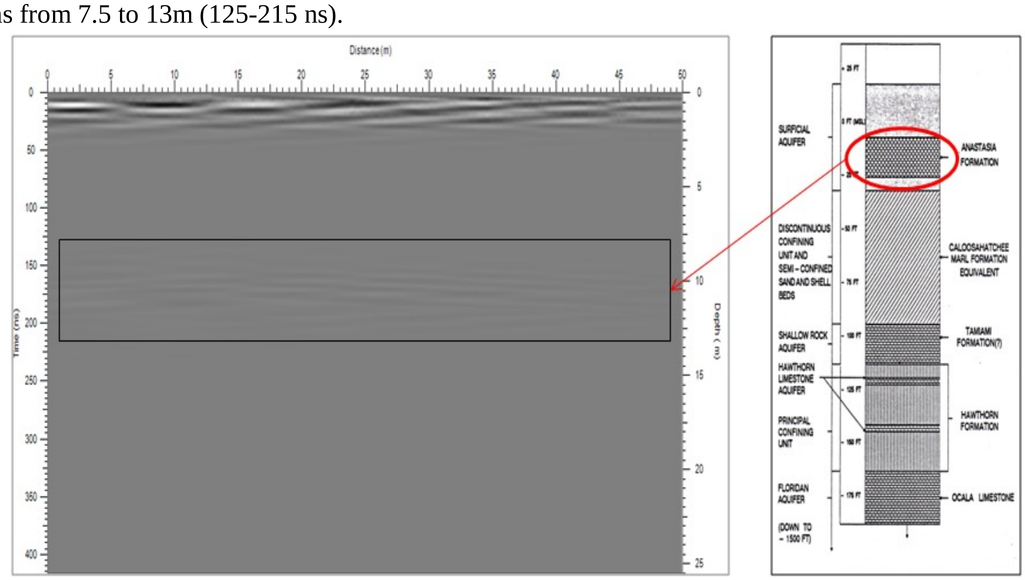

Source: *Adapted from Clark 1987*

Figure 4. GPR profile showing the location of the Anastasia formation.

Figure 5 shows three different GPR images from different elevations in the area surveyed. The first GPR profile was from the top of the ridge (highest elevation), the second profile was collected from the swale (lowest elevation) while the third profile was from the mid-ridge (mid-elevation). From the three profiles, the second profile collected from the swale or the low-lying area display some strong anomalous patterns through the entire profile as shown by the trace view of the profile. This is closely associated with the moisture content of the soil surveyed. The soil type in the area around where the image was taken is clay (on the swale). The velocity of propagation can vary within a soil type depending on local conditions of moisture content and material structure [9]. The penetrating depth to which the EM waves propagate is reduced by the conductivity of the media, in highly conductive media. The penetration depth is reduced as the percentage of clay increases in the soil [17] and explains the strong reflection and anomalous pattern evident in the GPR profile collected around the swale or low lying area. These findings were further supported by [18] who found that clay particles, like soil around the swale or low-lying areas, have high surface areas, water holding capacity, and cation exchange capacity all of which affect soil conductivity and result in an overall increase in signal attenuation.

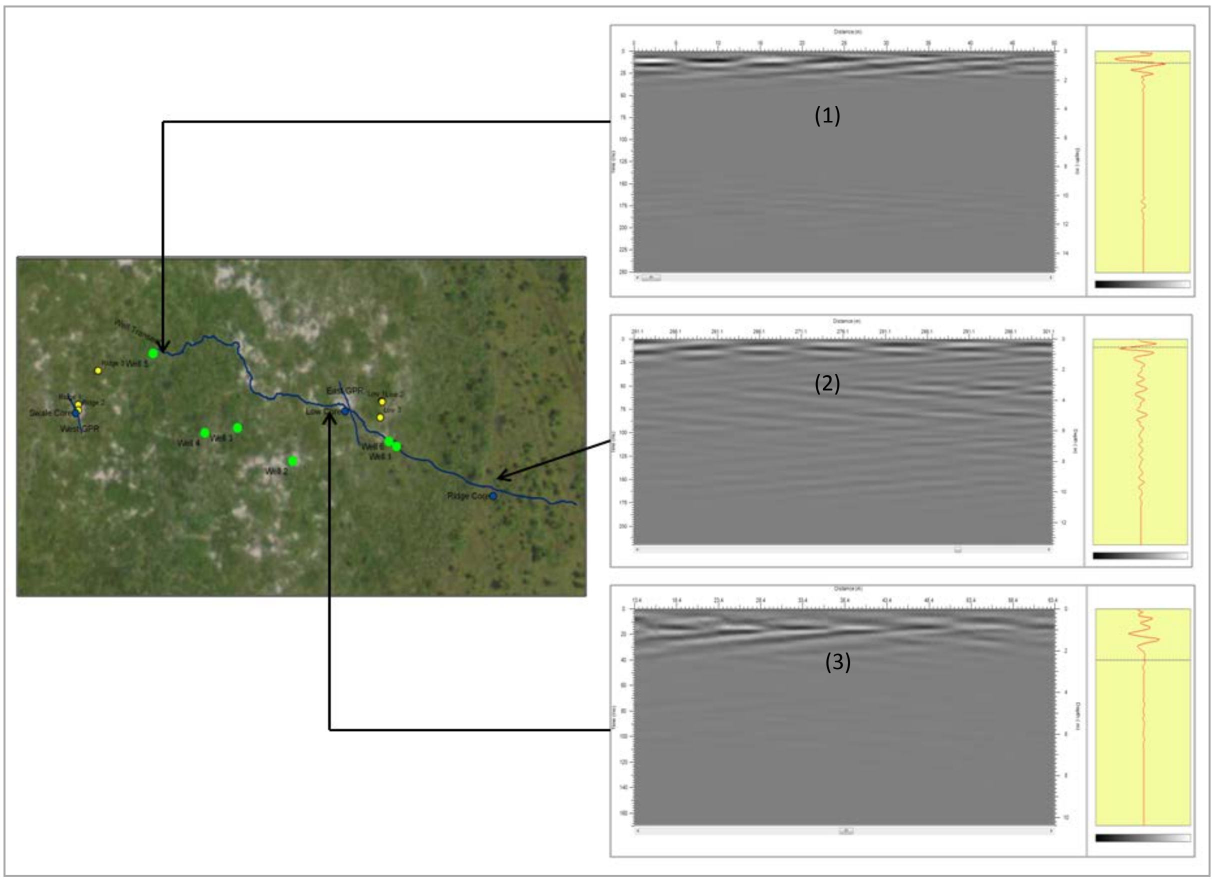

Figure 5. GPR profiles and trace window from different elevations along the GPR transect.

Figure 6 and 7 show the GPR profiles collected close to monitoring well-1 and well-5 respectively (marked by red dashed circle) on two different days. The location of the wells is shown in green dots on the same image. In both figures, depth to water table (marked by the solid red line) is shown around 1.5-2 m. From Figure 6, the depth to water table on 1/26/2012 was 1.5 m for well-1 measured directly in wells using the pressure sensitive data logger. From the same GPR profiles it can clearly be seen that the end of the strong continuous reflection marks the start of the depth to water table at 1.4 m, compared to what was measured from the monitoring well-1 on the same date, there seems to be a strong correlation between the GPR profile and monitoring wells.

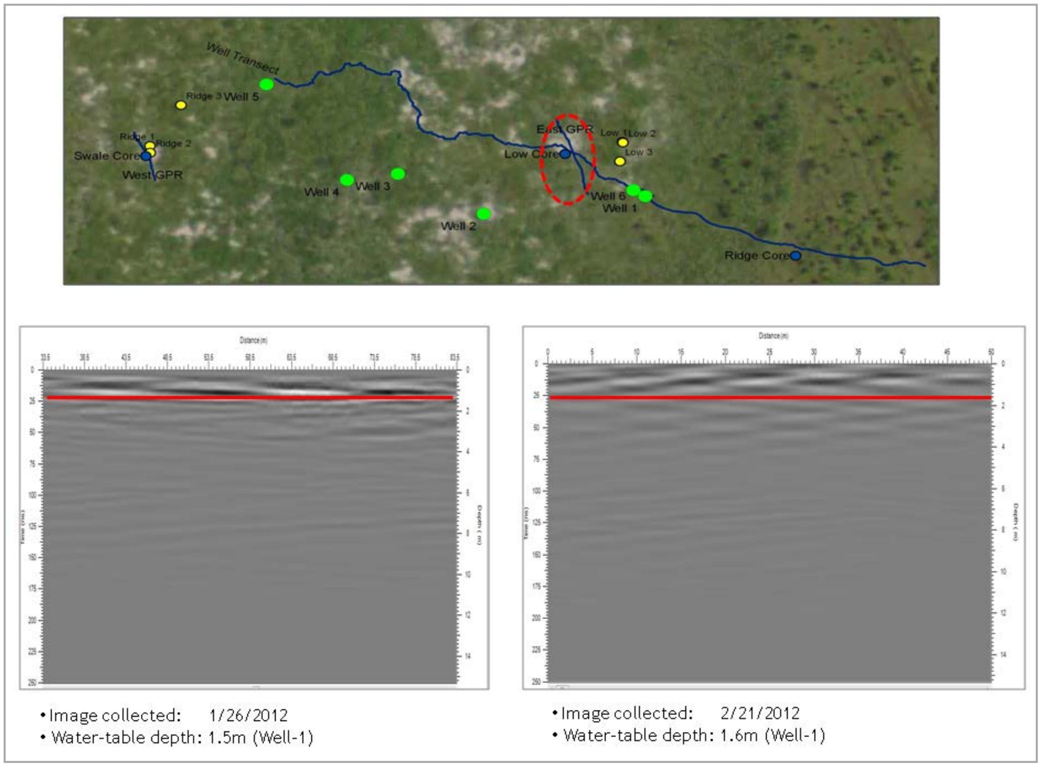

Figure 6. Radar at the top of ridge (mid-elevation). Red dashed circle denotes the area radar station.

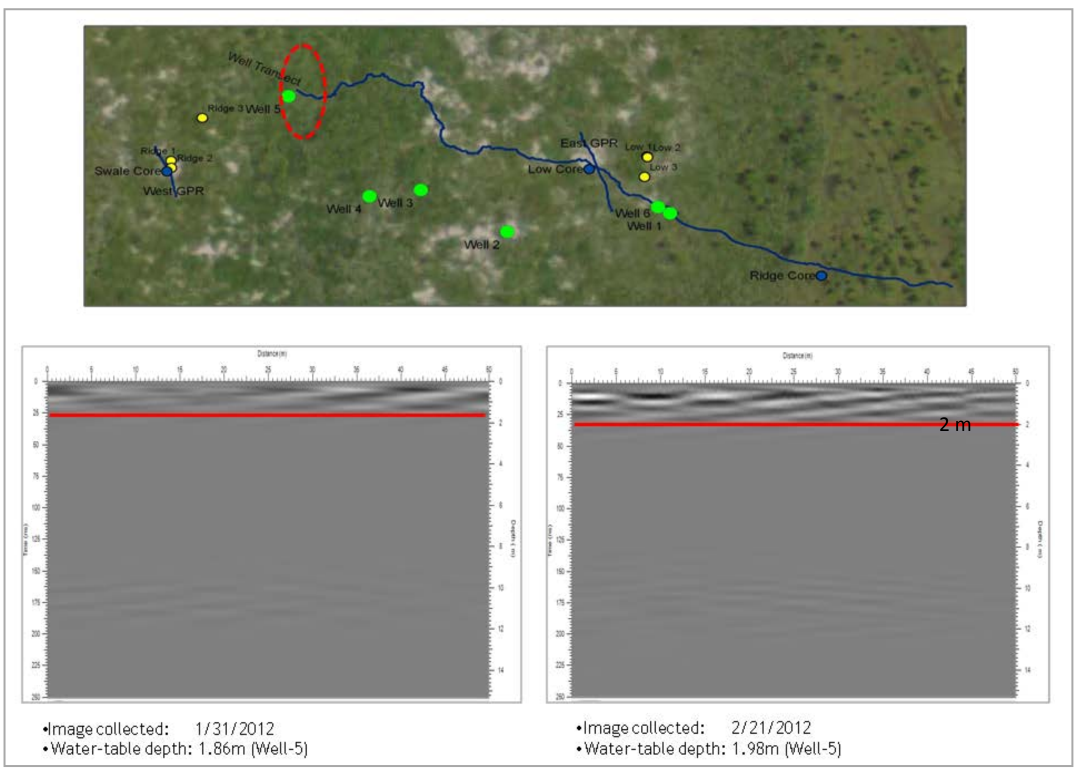

Figure 7. Radar from the top ridge (highest elevation). Red dashed circle denotes the area radar was collected.

[18], [19], [20] found good correlation between the radar estimated depth and manually (Monitoring wells or soil/snow auger) determined depth to water table. A study [19] in Patseo and Solang in the Himalayas to determine the snowpack properties (density, layer thickness and the layer type) using a 1000 MHz antenna. The study found a very good correlation between the manually measured and observed snow depth and the GPR estimated depth as shown in Figure 8a. Figure 8 (b) shows the linear correlation of this study. There was a correlation between the GPR estimated depth and monitoring wells or soil auger estimated depth with the correlation coefficient of $R^2 = 0.80$. This result demonstrates that 100 MHz antenna can locate depth to water table if ground truthing is conducted and suitable GPR processing software are used to process and analyze the data.

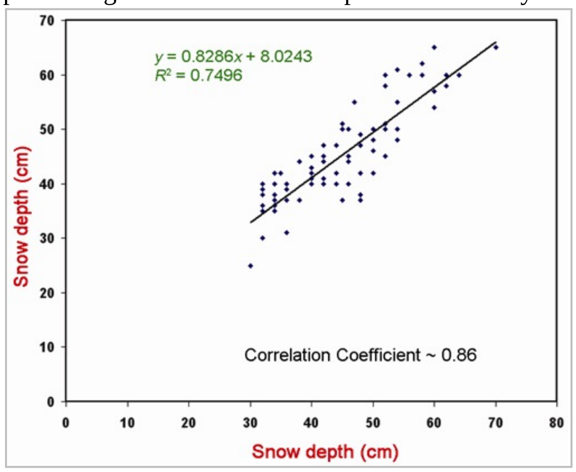

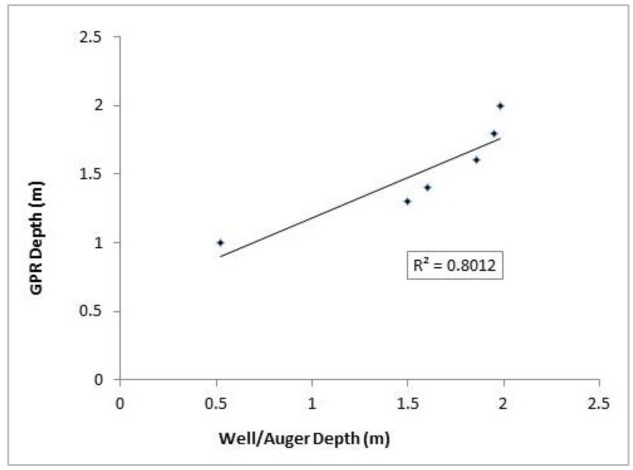

(a) Correlation coefficient [19]. (b) Correlation coefficient from our study.

Figure 8. Correlation between GPR estimated and measured depth to water/snow table.

The dominant sand at Tel-4 is well drained and belongs to the Order Spodosol. Two of the major soils found in scrub and Flatwoods at KSC are the Immokalee and Myakka.

Figure 9. Patches of bare highly leached white sand dominant at Tel-4.

Figure 10 shows the GPR profile taken after the soil auger was bored through a selected area on the mid-elevation to determine the subsurface features. The soil auger was used in randomly selected areas within the GPR transect to validate any ambiguous observations on the radar records obtained in the field and to confirm depth to water table and location of spodic horizon. This process was required at each site because soils have various dielectric properties (i.e., soil moisture, clay mineralogy, and others), which influence the two-way pulse travel time of the electromagnetic energy emitted. The upper interface or layer that mostly consisted of white highly leached sand seemed to be relatively shallow (<10 cm) when it was sampled with a soil auger. Immediately below the white sand was dark-colored dry peat and consisted of coarse and fine roots material, this extended for 1.2 m, after which the more wet peat with coarse and fine roots was encountered at 1.2 m (black solid line on GPR profile). The interfaces are taken to coincide with the spodic horizon which is rich in organic matter, iron, aluminum and some organo-complexes [21].

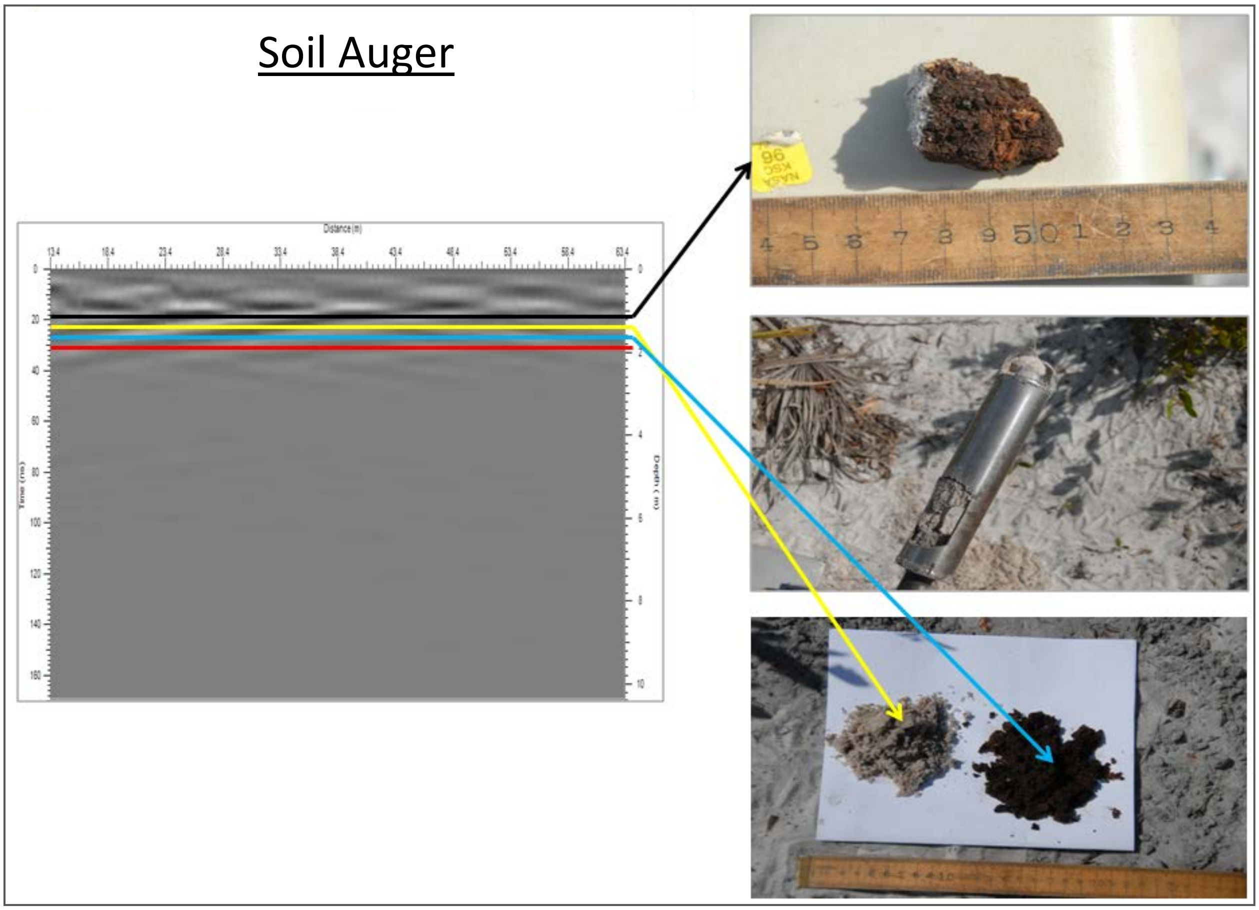

Figure 10. Water table depth and different soils as estimated by the soil auger.

The layer below the wet peat at 1.2 m was dry white sand encountered at 1.30 m represented by a yellow solid line on the GPR profile. There was no clear anomalous pattern representing this layer on the GPR profile. As shown in Figure 10 and indicated by blue solid line, dark wet soil with no fine or coarse roots were encountered at 1.50 m. This interface overlaid the water table depth; the more saturated zone was encountered at 1.95 m. Typically, GPR produces a time–distance record of the subsurface. In order to convert the time scale into a depth scale, the velocity of pulse propagation must be known. The most direct and accurate method to estimate the propagation velocity is to measure the two-way travel time to a reflector of known depth that appears on a radar image. In soils that have low electrical conductivity, the propagation velocity can be estimated using equation 1 and 2. Two-way travel time and signal propagation velocity to the water table depth of the same GPR profile was calculated and the result is shown in figure below.

Velocity analysis equation was used to determine the velocity of subsurface materials, then converting the reflection travel times to depths and validating with the soil auger. Using equation 1 and 2, the velocity to the interface interpreted as the water table depth was 0.13 ns and the calculated dielectric constant was 5.34 as shown in Figure 11. The average dielectric constant of soils in the study area determined using the Trase instrument was 4. The calculated dielectric constant was 5.34, because moist interfaces have higher dielectric constant, thus low waves velocity [10], consequently the velocity of electromagnetic waves propagating in the ground is decreased. The depth to the water table was again interpreted as the end of a more pronounced reflection at 2 m, and from the soil auger the depth to the water table was at 1.95 m.

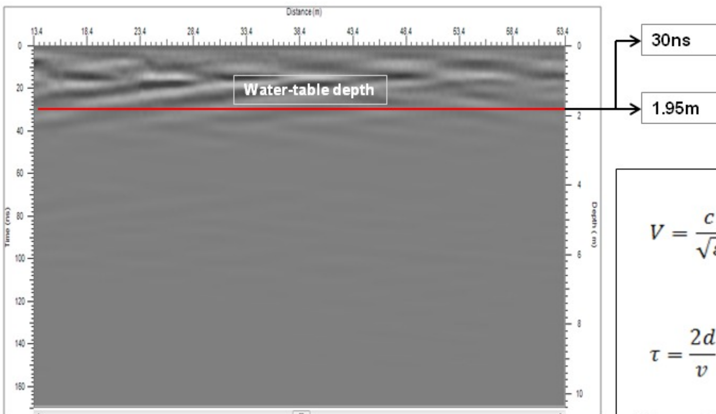

$$V = \frac{c}{\sqrt{\varepsilon}} \quad (1)$$

$$\tau = \frac{2d}{v}, \frac{2d\sqrt{\varepsilon}}{c} \quad (2)$$

Where, V is the wave velocity

C is speed of light (0.3 m/s)

$\mathcal{E}$ is dielectric constant of the soil

τ is two-way travel time

d is depth to the medium boundary

$$V = \frac{2d_w}{\tau_w} = \frac{2(1.95\ m)}{30\ ns} = 0.13\ m/ns$$

$$\sqrt{\varepsilon} = \frac{C}{V} = \frac{0.3\ m/ns}{0.13\ m/ns} = 2.31$$

$$\mathcal{E} = 5.34$$

Figure 11. GPR profile showing location of the water table depth and equations used to determine velocity, two-way travel time and dielectric constants.

6. SUMMARY AND CONCLUSION

Results indicate that GPR can be used as a viable methodology to detect subsurface features such as water table depth. The report has further demonstrated the ability of GPR to detect Holocene and Pleistocene depositional environments. The main disadvantage of GPR, however, is its poor penetration ability into electrically conductive material such as silt/clay deposits and saline saturated medium. In contrast, GPR was found to be most effective in terms of resolution, continuity of reflections and depth of penetration in dry sand. The study did not find any clear features on GPR profiles attributed to changes in soil moisture in the area, as well as location of the spodic horizon. This could be attributed to the coarse resolution of the 100 MHz antenna used in this study. To be able to detect features at the very top layer (within few centimeters) of the GPR profiles a higher frequency antenna can be used for finer resolution. The depth to water table was manually determined using pressure sensitive data logger in the shallow monitoring wells, and water table depth estimated using the soil auger had a good correlation with the estimated water table depth using GPR. Although we could collect only few data points with the GPR and soil auger, the water table depth was estimated with higher accuracy. The soil auger validated any ambiguous observations on the radar records obtained in the field and corroborated depth to water table with the GPR profiles.

Our frequent ground truthing through the use of soil auger and use of shallow monitoring wells in the area, and detailed analysis of the GPR profiles with GPRSoft software ensured accurate analysis and interpretation of GPR profiles. Accurate [18] and quantitative GPR measurements require frequent ground truth information to support features observed on the radar record.

7. ACKNOWLEDGEMENTS

InoMedic Health Application (IHA) provided Gideon the opportunity to conduct an internship under their sponsorship. The generous sponsorship from Fulbright Foundation, US Department of State is appreciated. Thanks are due to the Marine Environmental Optics Laboratory & Remote Sensing Center at Florida institute of Technology for constant guidance and supervision during Gideon's Fulbright fellowship and the research work at Kennedy Space Center.

REFERENCES

[1] Clark Engineers-Scientist, "KSC Subsurface Hydrology and Groundwater Survey-The Area wide Program". KSC-DF-3081. No. 97, (1987)

[2] Moreno-Casasola, P. and Vázquez, G., "The relationship between vegetation dynamics and water table in Tropical Dune Slacks", Journal of Vegetation Science, Vol. 10, no. 4, pp. 515-524 (1999)

[3] Hammersmark, C. T., Rains, M. C., Allison, W.C. and Jeffrey, M. F., "Vegetation and water-table relationships in a hydrologically restored riparian meadow". Wetlands. Vol. 29, no. 3, pp. 785–797, (2009)

[4] Bian, Z., Lei, S., Inyang, H.I., Chang, L., Zhang, R., and He, C. Z. X., "Integrated method of RS and GPR for monitoring the changes in the soil moisture and groundwater environment due to underground coal mining", Environ. Geol , Vol. 57, pp. 131–142 (2009)

[5] Bostater, C.R., Hall, C.R., Vleglais, D., Rebbman, J., and Provancha, M., "Temporal measurements of high resolution spectral signatures of plants and relationships indicating water status" In Proceeding of the International Symposium on Spectral Research (R.B. Gomez, Ed.), July 10-15, Volume I, San Diego, CA, pp. 387-402, (1994)

[6] Groenenboom, J., and Yarovoy, A., "Data Processing and Imaging in GPR System Dedicated for Landmine Detection", Subsurface Sensing Technologies and Applications. Vol. 3, no. 4, pp. 387-402, (2002)

[7] Lu, Q. and Sato, M. "Estimation of Hydraulic Property of an Unconfined Aquifer by GPR", Sens Imaging, vol. 8, pp. 83–99, (2007)

[8] Breininger, D. R., Duncan, B. W. and Dominy, N. J., "Relationships between fire frequency and vegetation type in pine Flatwoods of east-central Florida, USA". Natural Areas Journal. Vol. 22, pp.186–193 (2002)

[9] Jensen, J.R. "Remote Sensing of the Environment: An Earth Resource Perspective", Second edition, Upper Saddle River, New Jersey: Prentice Hall, 592 pp. (2007)

[10] Martinez, A. and Byrnes, A.P., "Modeling Dielectric-constant values of Geologic Materials: An Aid to Ground-Penetrating Radar Data Collection and Interpretation". Cur Res Earth Sci, Vol. 1, no. 1, pp. 11 (2001)

[11] Lunt, I.A., Hubbard,S.S. and Rubin, Y., "Soil moisture content estimation using ground-penetrating radar reflection data". Journal of Hydrology, Vol. 307, pp. 254–269 (2005)

[12] Daniels, D.J., Gunton. And Scott, H.F., “Introduction to subsurface radar”. IEE Proceedings, Vol. 135, Pt. F, No. 4, August 1988 (1988)

[13] ProEx-Operating Manual v. 2.0. (2011, November 13). [online]. Available: http://www.malags.com

[14] Shukla, S.B., Patidar, A.K. and Bhatt, N., “Application of GPR in the study of shallow subsurface sedimentary architecture of Modwa spit, Gulf of Kachchh”, Journal Earth Systems. Science. Vol. 117, no. 1, pp. 33–40, (2008)

[15] Annan, A.P., “Practical Processing of GPR data, Sensors and Software, Inc.” Mississauga, ON, Canada. (1999)

[16] Seger, M.A. and Nashait, A.F., “Detection of Water-Table by Using Ground Penetration Radar (GPR)”, Eng. & Tech. Journal, Vol. 29, no. 3, pp.: 554-566 (2011)

[17] Xeidakis, G.S., Torok, A., Skias, S. and Kleb, B., “Engineering Geological Problems Associated With Karst Terrains: Their Investigation, Monitoring, and Mitigation and Design of engineering Structures on Karst Terrains”, Bulletin of the Geological Society of Greece vol. XXXVI, 2004, Proceedings of the 10th International Congress, Thessaloniki, April 2004. (2004)

[18] Sucre, E.B., Tuttle, J.W. and Fox, T.R., "The Use of Ground-Penetrating Radar to Accurately Estimate Soil Depth in Rocky Forest Soils", Forest Science, Vol. 57, no. 1, pp. 59-66 (2011)

[19] Singh, K.K., Datt, P., Sharma, V., Ganju, A., Mishra, V.D., Parashar, A. and Chauhan, R., "Snow depth and snow layer interface estimation using Ground Penetrating Radar", Current Science, Vol. 100, no. 10, pp. 1532-1539 (2011)

[20] Doolittle, J.A., Jenkinson, B., Hopkin, D., Ulmer, M. and Tuttle, W., "Hydropedological investigations with ground-penetrating radar (GPR): Estimating water-table depths and local ground-water flow pattern in areas of coarse-textured soils", Geoderma, Vol. 131, pp. 317–329 (2006)

[21] Schmalzer, P.A. and Hinkle, G.A., “Geology, Geohydrology and Soils of the Kennedy Space Center: A Review. NASA Kennedy Space Center, FL”, (1990)